

ANALYSIS AND APPLICATIONS OF THE EXPONENTIAL TIME DIFFERENCING SCHEMES AND THEIR CONTOUR INTEGRATION MODIFICATIONS*

QIANG DU^{1,**} and WENXIANG ZHU¹

¹*Department of Mathematics, Pennsylvania State University, University Park,
PA 16802, USA. email: {qdu,zhu_w}@math.psu.edu*

Abstract.

We study in this paper the exponential time differencing (ETD) schemes and their modifications via complex contour integrations for the numerical solutions of parabolic type equations. We illustrate that the contour integration shares an added advantage of improving the stability of the time integration. In addition, we demonstrate the effectiveness of the ETD type schemes through the numerical solution of a typical problem in phase field modeling and through the comparisons with other existing methods.

AMS subject classification (2000): 65M15, 65M70, 82D99.

Key words: time integration schemes, exponential time differencing, contour integrals, Fourier spectral methods, stability, Fourier analysis, energy estimates, maximum principle, Allen–Cahn equations, phase transitions.

1 Introduction.

In an earlier work [7], we have studied some stability properties of the exponential time differencing schemes for some, mostly linear, parabolic equations. Our study was motivated by the increasing interests in recent years in using the phase field models in the computational material science [4, 11]. For many such models, for example, the time-dependent Ginzburg–Landau (TDGL) equations (or Allen–Cahn equations), Cahn–Hilliard equations, spectral and pseudo-spectral methods have been shown to provide remarkably effective spatial discretizations [5]. High order time integration schemes can be naturally combined with high resolution spectral schemes to provide efficient approximations of the phase field models. The ETD method, first studied by [6], is one of the many methods developed for solving stiff differential equations, see [12] for an comprehensive treatment. Of particular interests to us are the ETD and the modified ETD schemes for the diffusive type problems [6, 13]. It is hopeful that such techniques

* Received April 2004. Revised April 2005. Communicated by Anders Szepessy.

** This work is supported in part by grants NSF-DMS 0196522 and NSF-ITR 0205232.

may also be very useful in phase field computations that involve more complex physics.

In [7], we have illustrated various features of the ETD schemes (mostly limited to the first order ETD scheme) such as their stability and monotonicity. Naturally, in practice, the more interesting cases would be related to the higher order ETD schemes as well as their contour integral modifications proposed in [13]. In this continuing work, we make additional theoretical analysis including the derivation of a maximum principle for linear equations with shifts and for the nonlinear Allen–Cahn equation. Moreover, we investigate the effect of complex integration when these schemes are applied to solve some model parabolic equations. Until now, besides the results of [7], the stability of ETD schemes is only studied in [6] for ODEs, while the stability of the modified ETD scheme has not been touched upon in [13].

In our present work, we also make a direct numerical comparison of the modified ETD schemes of [13] with other methods that are popular in the solution of phase field models, for example, the semi-implicit method used by [5]. The comparison is based on the simulation of the two and three-dimensional TDGL equations which is often the first step towards a more realistic simulation of the phase field model in a binary alloy system [4].

The rest of the paper is organized as follows. In Section 2, we introduce the original and modified ETD schemes. We then turn to discuss the stability properties of those schemes for some model problems in Section 3. We also examine the effect of the contour complex integration and illustrate through a simple example that it improves the stability of the marching scheme. Some numerical experiments will be given in Section 4.

2 The exponential time differencing schemes.

We follow mostly the notation used in [7]. Given a linear elliptic operator \mathcal{L} , we consider the partial differential equation (PDE) for a scalar function u defined in a spatial domain $\Omega = [0, 2\pi]^d \subset \mathbb{R}^d$ and for time $t > 0$:

$$(2.1) \quad u_t = \mathcal{L}u + \mathcal{N}(u, \mathbf{x}, t),$$

along with suitable initial and boundary conditions with \mathcal{N} being a generic nonlinear term. Of particular interest to us is the dimensionless time-dependent Ginzburg–Landau (Allen–Cahn) equation:

$$(2.2) \quad u_t = \Delta u + \mathcal{N}(u),$$

with $\mathcal{N}(u) = u(1 - u^2)$, and Δ being the Laplace operator. It is also convenient to introduce a related linear equation of the type

$$(2.3) \quad u_t = \Delta u + \lambda u,$$

where λ can either be a constant or a function of time and the spatial variables. For most of our discussions, initial boundary value problems with either periodic

or homogeneous Dirichlet boundary conditions are considered for Equations (2.2) and (2.3).

Discretizing the PDE (2.1) in the spatial variables, for instance, by spectral approximations or by finite element approximations, a system of ordinary differential equations (ODEs) is often obtained

$$(2.4) \quad u_t = \mathbf{L}u + \mathbf{N}(u, t).$$

The exponential time differencing (ETD) methods can be described in the context of solving (2.4). Integrating the equation over a single time step from $t = t_n$ to $t = t_{n+1} = t_n + h$, we get

$$(2.5) \quad u(t_{n+1}) = e^{\mathbf{L}h}u(t_n) + e^{\mathbf{L}h} \int_0^h e^{-\mathbf{L}\tau} \mathbf{N}(u(t_n + \tau), t_n + \tau) d\tau.$$

Various ETD schemes come from the approximations to the integral in (2.5) [6].

If we denote the numerical approximation to $u(t_n)$ by u_n , then the first order scheme ETD1 is given by

$$(2.6) \quad u_{n+1} = e^{\mathbf{L}h}u_n + \mathbf{L}^{-1}(e^{\mathbf{L}h} - \mathbf{I})\mathbf{N}(u_n, t_n).$$

A second-order Runge–Kutta ETD scheme (ETDRK2) is given by

$$(2.7) \quad a_n = e^{\mathbf{L}h}u_n + \mathbf{L}^{-1}(e^{\mathbf{L}h} - \mathbf{I})\mathbf{N}(u_n, t_n),$$

$$(2.8) \quad u_{n+1} = a_n + h^{-1}\mathbf{L}^{-2}(e^{\mathbf{L}h} - \mathbf{I} - \mathbf{L}h)(\mathbf{N}(a_n, t_n + h) - \mathbf{N}(u_n, t_n)).$$

A third-order ETD Runge–Kutta scheme (ETDRK3) can be also found in [6], and the formulae for a fourth-order scheme (ETDRK4) are:

$$(2.9) \quad a_n = e^{\frac{\mathbf{L}h}{2}}u_n + \mathbf{L}^{-1}(e^{\frac{\mathbf{L}h}{2}} - \mathbf{I})\mathbf{N}(u_n, t_n),$$

$$(2.10) \quad b_n = e^{\frac{\mathbf{L}h}{2}}u_n + \mathbf{L}^{-1}(e^{\frac{\mathbf{L}h}{2}} - \mathbf{I})\mathbf{N}\left(a_n, t_n + \frac{h}{2}\right),$$

$$(2.11) \quad c_n = e^{\frac{\mathbf{L}h}{2}}a_n + \mathbf{L}^{-1}(e^{\frac{\mathbf{L}h}{2}} - \mathbf{I})\left(2\mathbf{N}(b_n, t_n + \frac{h}{2}) - \mathbf{N}(u_n, t_n)\right),$$

$$(2.12) \quad u_{n+1} = e^{\mathbf{L}h}u_n + h^{-2}\mathbf{L}^{-3}\left\{[-4 - \mathbf{L}h + e^{\mathbf{L}h}(4 - 3\mathbf{L}h + (\mathbf{L}h)^2)]\mathbf{N}(u_n, t_n) + [4 + 2\mathbf{L}h + 2e^{\mathbf{L}h}(-2 + \mathbf{L}h)] \times \right. \\ \times \left. \left(\mathbf{N}\left(a_n, t_n + \frac{h}{2}\right) + \mathbf{N}\left(b_n, t_n + \frac{h}{2}\right)\right) + [-4 - 3\mathbf{L}h - (\mathbf{L}h)^2 + e^{\mathbf{L}h}(4 - \mathbf{L}h)]\mathbf{N}(c_n, t_n + h)\right\}.$$

ETD schemes have also been used by other authors under different names [2, 16].

To overcome the vulnerability of error cancellations in the higher-order ETD and Runge–Kutta ETD schemes, and to generalize the ETD schemes to non-diagonal problems, in [13], modified ETD schemes are proposed by using the

complex contour integrals

$$(2.13) \quad f(\mathbf{L}) = \frac{1}{2\pi i} \int_{\Gamma} f(t)(t\mathbf{I} - \mathbf{L})^{-1} dt$$

to evaluate the coefficients in the formulae for ETDRK4. More detailed derivations and applications of the ETD and the modified ETD schemes can be found in [6, 13].

3 Analytical studies of the ETD and the modified ETD schemes.

Continuing the work in [7], we examine the stability and accuracy issues related to the ETD and the modified ETD schemes.

3.1 Pointwise bounds and monotonicity of the first order ETD scheme.

In [7], we studied the point-wise behavior of the first order ETD scheme for linear parabolic equations in one space dimension. Here, we extend the results to the case where a splitting technique is incorporated, and also to the case of the time-dependent Ginzburg–Landau (or Allen–Cahn) equation.

A simple semi-implicit splitting method for (2.1) over a single time step from t_n to $t_{n+1} = t_n + h$, can be described as follows:

$$\frac{\partial u}{\partial t} + \beta u = \mathcal{L}u + (\mathcal{N}(u(t_n), \mathbf{x}, t_n) + \beta u(t_n)),$$

where $\beta > 0$ is some positive constant and $t_n \leq t \leq t_{n+1}$. Note, when $\beta = 0$, $L = \mathcal{L}$ and $N = \mathcal{N}$, this corresponds to (2.6). Taking \mathcal{L} to be the Laplacian operator Δ and $\mathcal{N}(u, \mathbf{x}, t) = \lambda u$, in the sequel we will use the following equation for illustration,

$$(3.1) \quad \begin{cases} \frac{\partial}{\partial t} w(\mathbf{x}, t) + \beta w(\mathbf{x}, t) = \Delta w(\mathbf{x}, t) + (\lambda + \beta) u_n(\mathbf{x}), \\ w(\mathbf{x}, 0) = u_n(\mathbf{x}). \end{cases}$$

Here we solve in the time interval $0 \leq t \leq h$ and allow λ to vary with respect to \mathbf{x} but not to t . The equation is largely motivated by the use of semi-implicit splitting techniques for nonlinear equations where λu , to a certain degree, could be interpreted as a frozen coefficient approximation to possible nonlinearities. Note that in the case where $\mathcal{N}(u(t_n), \mathbf{x}, t_n) = c$ is a constant in (2.1), the first order splitted ETD scheme applied to (2.4) with $L = \Delta$ and $N(u, t) = \beta u + c$ in fact gives the exact solution.

Now considering the case λ being real, we have the following result:

THEOREM 3.1. *For the 1D initial value problem (3.1) with $\max_x \lambda \leq 0$ and $\beta > 0$, then*

- (i) *if $1 + t(2 \min_x \lambda + \beta) \geq 0$, and $u_n \geq 0$ for all x , then $w(x, t) \geq 0$ for all x ;*
- (ii) *if $1 + t(2 \min_x \lambda + \beta) \geq 0$, then $|w(x, t)| \leq \sup_{x \in R} |u_n(x)|$.*

PROOF. We have

$$(3.2) \quad w(x, t) = \int_R u_n(x - y) \left(\int_0^t (\lambda + \beta) e^{-\beta s} \Phi(y, s) \, ds + e^{-\beta t} \Phi(y, t) \right) dy,$$

where $\Phi(y, s) = e^{-|y|^2/4s} / (4\pi s)^{1/2}$. Using the following inequalities which was used in [7]:

$$(3.3) \quad \int_0^t \Phi(y, s) \, ds = (2\pi)^{-1/2} |y| \left(|y| \sqrt{2t} e^{-|y|^2/4t} - \int_{|y|/\sqrt{2t}}^\infty e^{-u^2/2} \, du \right) \leq 2t \Phi(y, t),$$

if $\lambda + \beta < 0$, one has

$$(3.4) \quad [e^{-\beta t} + 2(\lambda + \beta)t] \Phi(y, t) \leq \int_0^t (\lambda + \beta) e^{-\beta s} \Phi(y, s) \, ds + e^{-\beta t} \Phi(y, t) \leq \Phi(y, t),$$

note that $e^{-\beta t} \geq 1 - \beta t$, and hence

$$e^{-\beta t} + 2(\lambda + \beta)t \geq 1 + (2\lambda + \beta)t,$$

therefore from (3.4) and noticing that $\int_R \Phi(y, t) \, dy = 1$, we see that the theorem will follow if $1 + t(2\lambda + \beta) > 0$. □

We also have

COROLLARY 3.1 *For the 1D initial boundary value problem (3.1) with periodic boundary conditions, if λ is also periodic with $\max_x \lambda \leq 0$, then under the condition $1 + t(2 \min_x \lambda + \beta) \geq 0$, we have*

- (i) $w(x, t) \geq 0$ for $x \in (0, 2\pi)$ if $u_n \geq 0$ for all $x \in (0, 2\pi)$;
- (ii) $|w(x, t)| \leq \sup_{x \in (0, 2\pi)} |u_n(x)|$.

PROOF. Using the periodic extensions similarly in [7], and then the assertion follows exactly as in the proof of 3.1. □

Let u_n be the numerical solution at the time step n , we recall that a marching scheme is called asymptotically B stable for some Banach space B if $\|u_{n+1}\|_B \leq \|u_n\|_B$ for all n . If no restriction needs to be imposed on the time step $\tau = t_{n+1} - t_n$ to achieve such stability bound, then the scheme is called unconditionally asymptotically B stable. For more discussion on the stability of numerical schemes, we refer to [12, 15].

The above results imply that a suitable splitting of the first order ETD scheme can improve its asymptotic L^∞ -stability for one-dimensional linear parabolic equations. This is consistent with the similar observations made in [7] on the L^2 -stability.

Next, some analysis on a model nonlinear equation, namely the time dependent Ginzburg–Landau Equation (2.2), is considered. The application of the first order ETD scheme to (2.2) leads to:

$$(3.5) \quad \begin{cases} \frac{\partial}{\partial t} w(\mathbf{x}, t) = \Delta w(\mathbf{x}, t) + u_n(\mathbf{x})(1 - u_n^2(\mathbf{x})), \\ w(\mathbf{x}, 0) = u_n(\mathbf{x}), \end{cases}$$

In the one-dimensional case, we have

$$(3.6) \quad w(x, t) = \int_0^t \int_R (u_n(x-y) - u_n^3(x-y)) \Phi(y, s) dy ds + \int_R u_n(x-y) \Phi(y, t) dy.$$

If $-1 \leq u_n(x) \leq 1$, we have

$$(3.7) \quad -2(1 + u_n) \leq u_n - u_n^3 \leq 2(1 - u_n),$$

then using (3.3), we have

$$(3.8) \quad \int_R (u_n(x-y) - 4t(1 + u_n(x-y))) \Phi(y, t) dy \leq w(x, t)$$

and

$$(3.9) \quad w(x, t) \leq \int_R (u_n(x-y) + 4t(1 - u_n(x-y))) \Phi(y, t) dy.$$

Therefore, if $1 - 4t \geq 0$, namely, $t \leq 1/4$, from (3.8) and (3.9), we will have $-1 \leq w(x, t) \leq 1$. This can be summarized as follows:

THEOREM 3.2. *For the first order ETD scheme for the 1D TDGL equation (3.5) with periodic boundary condition, if $-1 \leq u_n(x) \leq 1$ and if $t \leq 1/4$, then $-1 \leq w(x, t) \leq 1$.*

We note that Equation (3.5) is in a dimensionless form, thus, in practice, the stability condition $t \leq 1/4$ may vary according to the scales involved in the problem. At the moment, the maximum principle type results have been limited to only the one-dimensional space case.

3.2 Modified ETD scheme: effect of complex integral on stability.

One of the essential features of the modified ETD schemes proposed by [13] is the introduction of complex integral for the evaluations of the various solution operators (the semi-groups) related to the linear part. We note that it has been pointed out in [13] that normally a 32-point integration rule would suffice in most applications due to the high spectral accuracy of the quadrature. The stability of such a high precision rule would naturally be essentially the same as that with

an exact integration, which mathematically is equivalent to the original ETD schemes though the effect on the numerical computation due to rounding errors may be very different. The latter is in fact the motivation of the modification to the ETD schemes introduced in [13]. To carefully examine the role of numerical integration beyond its advantage of avoiding significant error cancellation in the actual implementation, we elect to consider the case of using just two points to perform the contour integrals. Though it may seem too simple-minded at first to examine such a case, it turns out that this modified scheme serves as a good example to reveal the effect of the complex integration on the numerical scheme, both in terms of stability and in terms of accuracy. It is then not hard for one to extrapolate and to understand the effect of higher order quadrature rules on higher order ETD schemes. Moreover, as shown later, although a two-point quadrature may not be highly accurate for the contour integral evaluation, the resulting time-marching scheme in fact enjoys improved stability and accuracy.

First of all, we recall that the two-point quadrature amounts to the approximation:

$$L^{-1}(e^{Lt} - 1) \sim \frac{1}{2}((L + ri)^{-1}(e^{(L+ri)t} - 1) + (L - ri)^{-1}(e^{(L-ri)t} - 1)).$$

THEOREM 3.3. *Assume that λ is a real number, if $\lambda < 0$, then the first order modified ETD scheme applied to Equation (2.3) using a two-points approximation of complex contour integral is asymptotically L^2 -stable for $t \leq \min(-2/\lambda, \pi/r)$.*

PROOF. Noticing that the application of the Fourier transform to (2.3) turns $L = \Delta$ into a diagonal operator, and e^L is also diagonal if L is, we thus only need to carry out a mode-wise analysis here. Denote $c_{\mathbf{k}} = -|\mathbf{k}|^2$ for $\mathbf{k} \in \mathbb{Z}^d$, where \mathbb{Z} denotes the set of integers, and \mathbf{k} is a Fourier mode. For each contour which is taken as a circle centered at $c_{\mathbf{k}}$ with radius $r > 0$, ri and $-ri$ are chosen as the quadrature points for the approximation of the contour integral. As in the case of the original ETD schemes, we can write

$$\begin{aligned} (3.10) \quad \widehat{w}_{\mathbf{k}}(t) &= e^{c_{\mathbf{k}}t} u_n + \frac{1}{2} \left(\frac{e^{(c_{\mathbf{k}}+ri)t} - 1}{c_{\mathbf{k}} + ri} + \frac{e^{(c_{\mathbf{k}}-ri)t} - 1}{c_{\mathbf{k}} - ri} \right) \lambda u_n \\ &= h(c_{\mathbf{k}}, t) u_n, \end{aligned}$$

where

$$(3.11) \quad h(\xi, r, t) \stackrel{\text{def}}{=} \frac{e^{\xi t}(r^2 + \xi^2 + \lambda \xi \cos(rt) + \lambda r \sin(rt)) - \lambda \xi}{\xi^2 + r^2},$$

and $\xi = c_{\mathbf{k}}(t)$. For convenience, let $x = -\xi t$, $y = -\lambda t$, and $\rho = rt$, then (3.11) can be written as

$$h(x, y, \rho) = \frac{e^{-x}(\rho^2 + x^2 + xy \cos \rho - y\rho \sin \rho) - xy}{x^2 + \rho^2},$$

and asymptotic L^2 -stability is equivalent to having $|h(x, y, \rho)| \leq 1$, namely,

$$(3.12) \quad p(x, y, \rho) \stackrel{\text{def}}{=} e^{-x}(\rho^2 + x^2 + xy \cos \rho - y\rho \sin \rho) - xy - x^2 - \rho^2 \leq 0,$$

and

$$(3.13) \quad \begin{aligned} q(x, y, \rho) &\stackrel{\text{def}}{=} e^{-x}(\rho^2 + x^2 + xy \cos \rho - y\rho \sin \rho) - xy + x^2 + \rho^2 \\ &= (\rho^2 + x^2)(e^{-x} + 1) + ye^{-x}(x \cos \rho - \rho \sin \rho - xe^x) \\ &\geq 0. \end{aligned}$$

First, note that if $x > 0$, $y > 0$, and $0 \leq \rho \leq \pi$, then

$$(3.14) \quad p(x, y, \rho) \leq (\rho^2 + x^2)(e^{-x} - 1) + xy(e^{-x} \cos \rho - 1) \leq 0,$$

and hence (3.12) holds. Secondly, note that $xe^x + \rho \sin \rho - x \cos \rho \geq 0$ for $x > 0$ and $0 \leq \rho \leq \pi$, and $t \leq -2/\lambda$ is equivalent to $y < 2$, so

$$e^x q(x, y, \rho) \geq (\rho^2 + x^2)(1 + e^x) - 2(xe^x + \rho \sin \rho - x \cos \rho) \stackrel{\text{def}}{=} f(\rho, x).$$

Let $g(x) = x(1 + e^x) - 2e^x + 2$. Note that $g(0) = 0$, and

$$\frac{dg}{dx} = e^x(e^{-x} + x - 1) > 0,$$

therefore $g(x) > 0$ for $x > 0$; and hence $f(0, x) = xg(x) > 0$. Noting that

$$\begin{aligned} \frac{\partial f}{\partial \rho} &= 2\rho(1 + e^x) - 2 \sin \rho - 2\rho \cos \rho - 2x \sin \rho \\ &\geq 2\rho(2 + x) - 2 \sin \rho - 2\rho \cos \rho - 2x \sin \rho \\ &\geq 2(1 + x)(\rho - \sin \rho) + 2\rho(1 - \cos \rho), \end{aligned}$$

and $\rho - \sin \rho > 0$ for $\rho > 0$, so $\partial f / \partial \rho > 0$ for $\rho > 0$ and $x > 0$. This implies that for any $x > 0$ and $0 < \rho \leq \pi$, we have $f(\rho, x) \geq f(0, x) > 0$. The theorem thus follows. \square

We note that the conditions on t in the above theorem are the same as those needed for the asymptotic L^2 -stability of the original first order ETD scheme without the contour integration.

Next, we consider the effect of the operator splitting on the modified ETD scheme. With a splitting of the term λu in Equation (2.3), the modified ETD scheme gives:

$$(3.15) \quad \begin{cases} \frac{\partial}{\partial t} w(\mathbf{x}, t) = (\Delta - \alpha)w(\mathbf{x}, t) + (\lambda + \alpha) u_n(\mathbf{x}), \\ w(\mathbf{x}, 0) = u_n(\mathbf{x}) \end{cases}$$

for some $\alpha > 0$. Following along the same line of discussion as in the above, we have

COROLLARY 3.2 *Assume that $\lambda < 0$, if $\alpha > -\lambda$ or if $0 < \alpha < -\lambda$ and $t \leq \min(-2/(\lambda + \alpha), \pi/r)$, then the first order ETD scheme with two-point complex integral approximation is asymptotically L^2 -stable.*

The stability conditions involved in Corollary 3.2 improve upon those obtained for the operator splitting of the original first order ETD scheme given in [7]. In comparison, we see that the complex contour integration generally not only helps reducing the error cancellation in the numerical implementation, but as our simple analysis indicates, it also has the added effect of improving the numerical stability of the marching scheme. This is already evident in the scheme based on a simple two point contour integration.

3.3 Modified ETD scheme: effect of complex integral on truncation error.

To study the local truncation errors of the first order ETD scheme with two-point complex integration, we consider its application to (2.3). Note that for the modified ETD schemes discussed in [13], the number of quadrature points is of the order of 32 and thus a larger contour radius is possible (and desirable for error cancellation reasons). For the two-point quadrature used an illustration here, the integration radius should not be too large, or we lose the accuracy of the scheme. Thus, we focus on the effect for contour radius, r , that is not too large.

The original first order ETD scheme without any complex integration has a corresponding symbol g which

$$\begin{aligned}
 (3.16) \quad g(\xi, t) &\stackrel{\text{def}}{=} 1 + \frac{e^{\xi t} - 1}{\xi}(\lambda + \xi) \\
 &= 1 + (\lambda + \xi)t + \frac{1}{2}\xi(\lambda + \xi)t^2 + \frac{1}{6}(\lambda\xi^2 + \xi^3)t^3 + \\
 &\quad + \frac{1}{24}(\lambda\xi^3 + \xi^4)t^4 + \mathcal{O}(t^5),
 \end{aligned}$$

and for the exact solution, we have

$$\begin{aligned}
 (3.17) \quad e^{(\lambda+\xi)t} &= 1 + (\lambda + \xi)t + \frac{1}{2}(\lambda + \xi)^2t^2 + \frac{1}{6}(\lambda + \xi)^3t^3 + \\
 &\quad + \frac{1}{24}(\lambda + \xi)^4t^4 + \mathcal{O}(t^5).
 \end{aligned}$$

Therefore, in general, without complex integration, the local truncation error of the first order ETD scheme is second order in t , the time step size.

Similarly, by using the Taylor series expansions in both t and r , we see that the modified ETD scheme shares the symbol:

$$\begin{aligned}
 (3.18) \quad h(\xi, r, t) &= 1 + (\lambda + \xi)t + \frac{1}{2}\xi(\lambda + \xi)t^2 + \frac{1}{6}(\lambda\xi^2 - \lambda r^2 + \xi^3)t^3 + \\
 &\quad + \frac{1}{24}(\lambda\xi^3 - 3\lambda\xi r^2 + \xi^4)t^4 + \mathcal{O}(r^2t^5).
 \end{aligned}$$

We see that generally, the modified scheme is also second order in the time step size for not so large r . For a fixed ξ (or a fixed Fourier mode), by choosing a large r , say $r = \sqrt{-3(\lambda + \xi)/t}$, one can have third order truncation error in t .

This improved accuracy has also been verified in our numerical implementation. However, for different Fourier modes, one would need to use different values of r . To conclude, we see that r does not greatly affect the order of local truncation error in general.

3.4 Analysis of higher order schemes.

We note that much of our discussions made in this sections have been primarily concerned with the first order ETD schemes or its modifications. Extensions to higher order schemes such as ETDRK3 and ETDRK4 are possible while the analytical derivations become much complex.

For instance, the application of ETDRK2 to (2.3) is equivalent to

$$u_{n+1} = (e^{Lh} + \lambda h^{-1} L^{-2}(e^{Lh} - I)^2 + \lambda^2 h^{-1} L^{-3}(e^{Lh} - I - Lh)(e^{Lh} - I))u_n.$$

Let $y = -\lambda h$ and $\xi = |\mathbf{k}|^2 h$, with \mathbf{k} being the Fourier modes, the corresponding amplification factor is

$$g_2(\xi, y) = \begin{cases} 1 - y + \frac{y^2}{2}, & \text{if } \xi = 0, \\ e^{-\xi} - y \frac{(e^{-\xi} - 1)^2}{\xi^2} + y^2 \frac{(e^{-\xi} - 1 + \xi)(1 - e^{-\xi})}{\xi^3}, & \text{if } \xi > 0. \end{cases}$$

For a given $\xi > 0$, direct computation shows that

$$\frac{\partial^2 g_2(\xi, y)}{\partial y^2} = 2 \frac{(e^{-\xi} - 1 + \xi)(1 - e^{-\xi})}{\xi^3} \geq 0,$$

and we can obtain that the minimum of $g_2(\xi, y)$ with respect to y is given by

$$h_2(\xi) \stackrel{\text{def}}{=} e^{-\xi} - \frac{1}{4} \frac{(1 - e^{-\xi})^3}{(e^{-\xi} - 1 + \xi)\xi}.$$

By the elementary inequality,

$$\xi e^\xi - \xi \geq 1 - e^\xi + \xi e^\xi \geq \frac{1}{2}(\xi e^\xi - \xi) \geq 0,$$

we have

$$\begin{aligned} h_2(\xi) &\geq e^{-\xi} - \frac{1}{4} \frac{(e^\xi - 1)^3}{e^{2\xi}(\xi e^\xi - e^\xi + 1)\xi} \\ &\geq e^{-\xi} - \frac{1}{2} \frac{(e^\xi - 1)^2}{e^{2\xi}\xi^2} \\ &\geq e^{-\xi} - \frac{1}{2} \geq -1. \end{aligned}$$

On the other hand, we have for $\xi > 0$,

$$g_2(\xi, 2) - 1 = \frac{1 - e^{-\xi}}{\xi^3} (4(e^{-\xi} - 1 + \xi) - 2\xi(1 - e^{-\xi}) - \xi^3).$$

Direct calculation shows that

$$4(e^{-\xi} - 1 + \xi) - 2\xi(1 - e^{-\xi}) - \xi^3 \leq 0,$$

which leads to $g_2(\xi, 2) \leq 1$. Since $g_2(\xi, 0) = e^{-\xi} \leq 1$, we see that $g_2(\xi, y) \leq 1$ for $y \in (0, 2)$. Thus, we have proved the following theorem:

THEOREM 3.4. *For the second order ETD scheme (2.7) for Equation (2.3) with periodic boundary condition and constant coefficient $\lambda \leq 0$, if $h \leq -2/\lambda$, then it is asymptotically L^2 -stable.*

For ETDRK3, let $p = e^{-\xi/2}$, $g_a = p + (y/\xi)(p - 1)$, $g_b = p^2 + \frac{y}{\xi}(p^2 - 1)(2g_a - 1)$, $A_3 = -4 + \xi + p^2(4 + 3\xi + \xi^2)$, $B_3 = 2 - \xi - p^2(2 + \xi)$, $C_3 = -4 + 3\xi - \xi^2 + p^2(4 + \xi)$, the amplification factor $g_3(\xi, y)$ is defined as

$$g_3(\xi, y) = \begin{cases} 1 - y + \frac{y^2}{2} - \frac{y^3}{6}, & \text{if } \xi = 0, \\ \tilde{g}_3(\xi, y) = p^2 + \frac{y}{\xi^3}(A_3 + 4B_3g_a + C_3g_b), & \text{if } \xi > 0. \end{cases}$$

In Figure 3.1(a), a surface plot of $\tilde{g}_3(\xi, y)$ is given for $\xi \in [0.001, 4]$ and $y \in [0, 2]$. It can be seen that the maximum value of $\tilde{g}_3(\xi, y)$ occurs at $y = 0$ and $\xi = 0.001$, while the minimal value is greater than -1 , and there are no other extreme values inside the ξ - y domain $[0.001, 4] \times [0, 2]$. Moreover, direct computation gives $\lim_{\xi \rightarrow 0} \tilde{g}_3(\xi, y) = 1 - y + y^2/2 - y^3/6$, which obtains maximum value 1 at $y = 0$ and a minimal value which is greater than -1 at $y = 2$. In addition to this, using the Taylor series expansions, we have $\lim_{\xi \rightarrow 0} \partial_\xi \tilde{g}_3(\xi, y) = -1 + y - y^2/2$, which is equal to -1 if $y = 0$; and $\lim_{\xi \rightarrow 0} \partial_y \tilde{g}_3(\xi, y) = -1$. Therefore the absolute value of the amplification factor $g_3(\xi, y)$ obtains the maximum value 1 for $y \in [0, 2]$.

For ETDRK4, similarly as in the case of ETDRK3, we can define the amplification factor $\tilde{g}_4(\xi, y)$ for $\xi > 0$ (while if $\xi = 0$, the amplification factor is $1 - y + y^2/2 - y^3/6 + y^4/24$). It can also be shown that $\lim_{\xi \rightarrow 0} \tilde{g}_4(\xi, y) = 1 - y +$

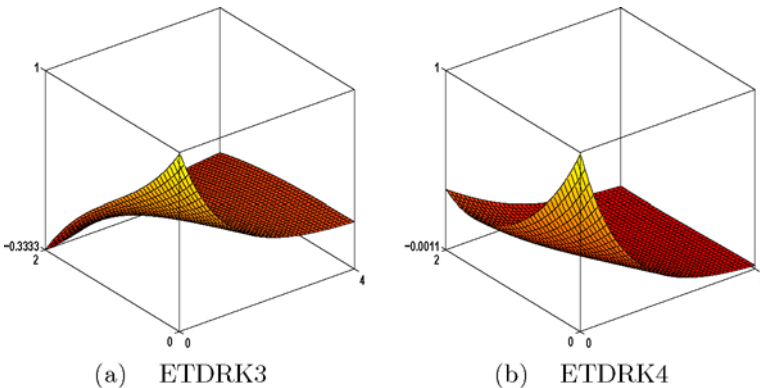


Figure 3.1: Surface plots of the amplification factors for ETDRK3 and ETDRK4.

$y^2/2 - y^3/6 + y^4/24$, and $\lim_{\xi, y \rightarrow 0} \partial_\xi \tilde{g}_4(\xi, y) = -1$, and $\lim_{\xi, y \rightarrow 0} \partial_y \tilde{g}_4(\xi, y) = -1$, and the absolute value of the amplification factor obtains the maximum value 1 for $y \in [0, 2]$ at $y = 0$ and $\xi = 0$ (also see Figure 3.1(b)). Thus, if $y = -\lambda h \in [0, 2]$, the maximal value of the absolute values of the amplification factors for ETDRK3 and ETDRK4 are no more than 1, and we have the following remark:

REMARK 3.1. For the higher order ETD schemes ETDRK2, ETDRK3, and ETDRK4 applied to Equation (2.3) with the periodic boundary condition and a constant coefficient $\lambda \leq 0$, if $h \leq -2/\lambda$, then the arguments above strongly suggest that they are asymptotically L^2 -stable.

3.5 Stability regions.

We define the stability regions as the parameter regions such that the magnitude of the amplification factor being no larger than 1 when applied to the model linear equation, which comes from the linearization of Equation (2.4):

$$(3.19) \quad u_t = \mathbf{L}u + \lambda u$$

with $\mathbf{L}u = \xi u$. In general, the parameters ξ and λ may both be complex-valued. We will first consider the case when λ is complex valued and ξ is a negative real number that corresponds to a Fourier mode of the operator \mathbf{L} that is self-adjoint and elliptic.

Since in solving PDEs, the intersections of the stability regions corresponding to different modes are most relevant, so we first present a picture of the stability regions of modified ETDRK4 with different values of ξt , see Figure 3.2. It can be seen that these regions share a nontrivial intersection which gives the region of stability for the original PDE.

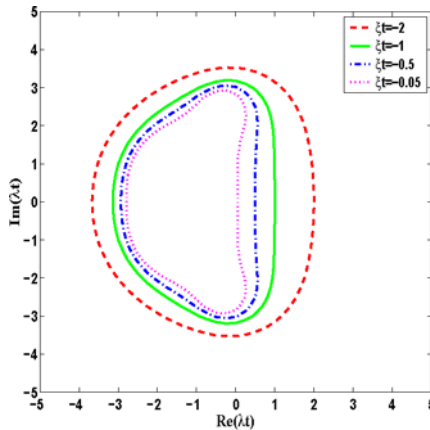


Figure 3.2: Stability regions of modified ETDRK4 in the complex plane of λt for $\xi t = -2, -1, -0.5$, and -0.05 (all using 32 nodes and a circle of radius 1 for complex contour integration).

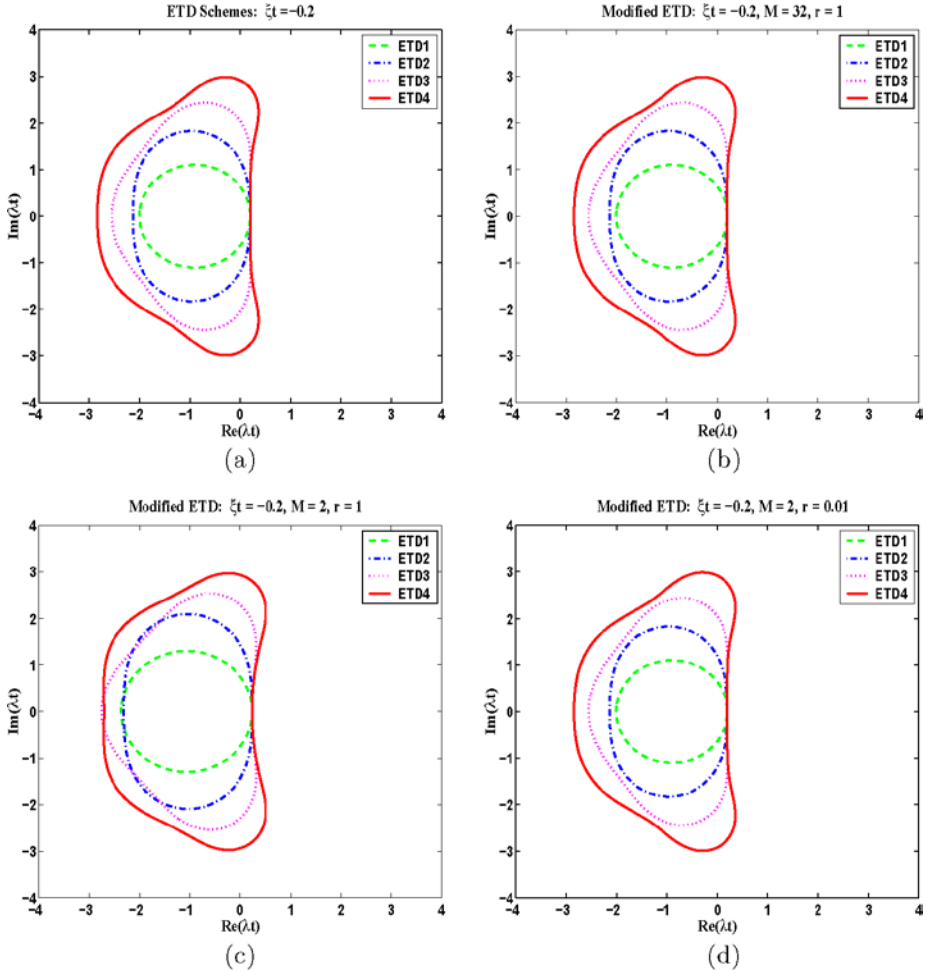


Figure 3.3: Stability regions for ETD and modified ETD schemes in the complex planes of λt , where $\xi t = -0.2$.

We then turn to investigate how numerical quadratures in the modified ETD schemes will affect the stability region for a single mode (a fixed value of ξ) since the complex integration can be done independently for different Fourier mode. Given $-\xi t = 0.2$, the stability regions of the ETD1, ETD2, ETD3, and ETD4 are shown in Figure 3.3(a), while the stability regions of the corresponding modified ETD schemes are shown in Figures 3.3(b)–(d) respectively. Let M be the number of integration nodes and r be the integration radius. In Figures 3.3(b)–(d), we have $M = 32, 2, 2$ and $r = 1, 1, 0.01$ respectively. Notice that Figures 3.3(a) and 3.3(d) are almost identical. Thus, it is seen that modified scheme with a good enough quadrature will have essentially the same stability regions as that of the original scheme. For small radius $r = 0.01$, even the two point quadrature gives regions close to that for the original ETD schemes. But

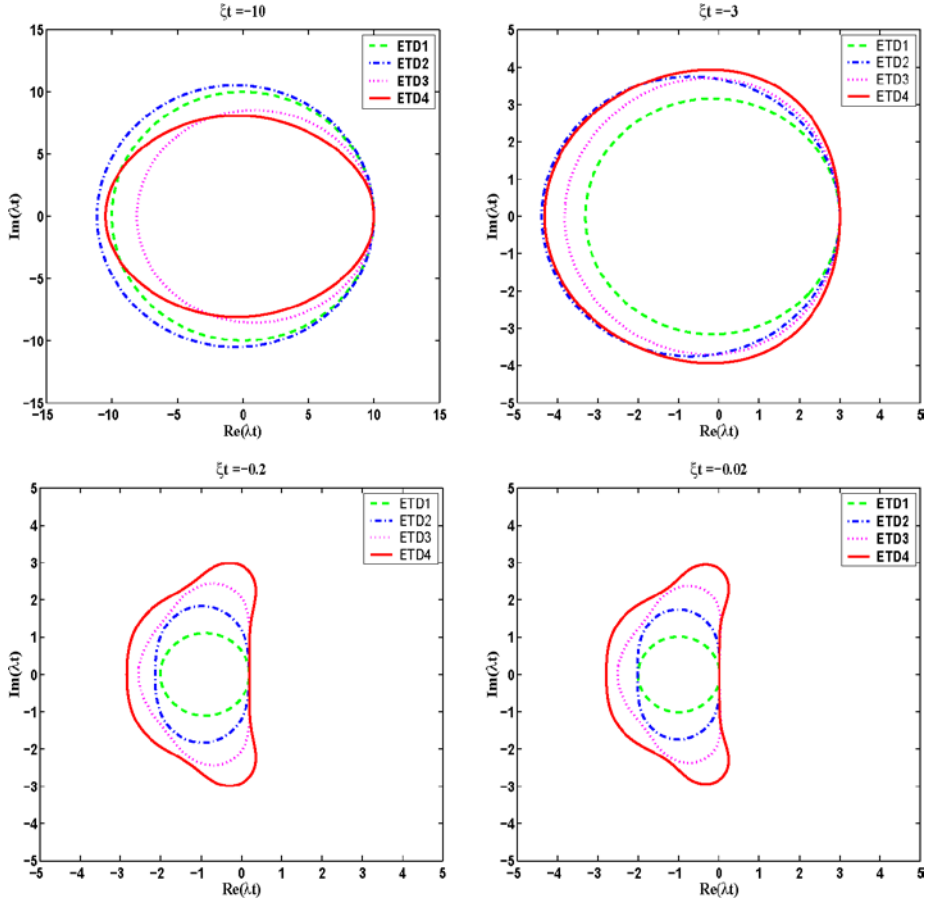


Figure 3.4: Stability regions for modified ETD schemes in the complex planes of λt for different values of ξt .

note that, however, in Figure 3.3(c), with $M = 2, r = 1$, the stability regions are different from those of the other figures.

The stability regions in the complex plane of λ for the modified ETD schemes (ETD1, ETDRK2, ETDRK3, and ETDRK4) are shown in Figure 3.4 for several given values of ξ with $M = 32$ and $r = 1$. Again, these regions are almost identical to those of the original ETD1, ETDRK2, ETDRK3 and ETDRK4 schemes. We observe that when $-\xi t > 0$ is large, the stability regions of the higher order ETD schemes (ETDRK3, ETDRK4) contain those of lower order ETD schemes; however, when $-\xi t > 0$ is small, they are contained by those of the lower order schemes instead. Such a fact has not been discussed in the literature [6]. Utilizing this observation in actual numerical implementation remains to be studied further.

Next, for λ and ξ both being real numbers, Figure 3.5 shows that the stability regions in the $\lambda t, \xi t$ plane for the four ETD schemes and their modifications with

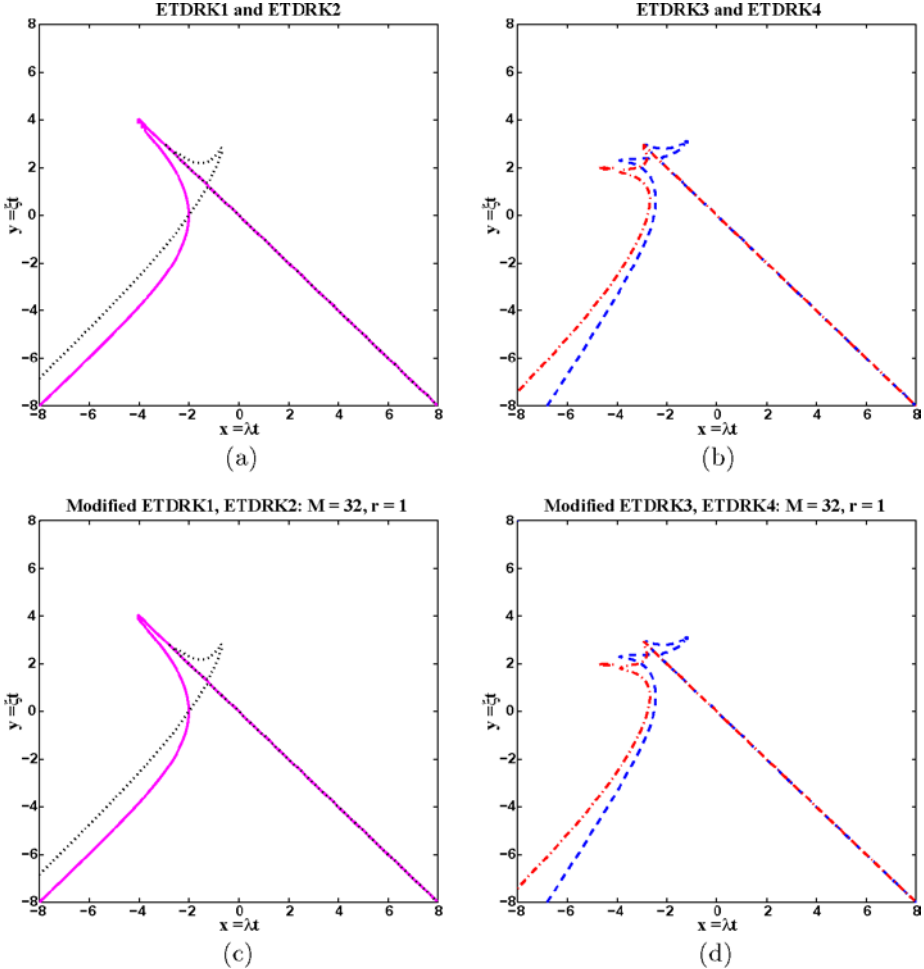


Figure 3.5: Stability regions of the ETD ((a)–(b)) and modified ETD schemes ((c)–(d)). In (a) and (c), solid line – ETD1, dotted line – ETD2; while in (b) and (d), dashed line – ETD3; dashed dotted line – ETD4. (In each plot, along the line $y = -x$, part of the two curves match, and it is hard to tell the difference between them.)

complex contour integrals, where $M = 32$ quadrature points on a unit circle are taken. We only display the domain where λt and ξt are in $[-8, 8]$. The similarity of the stability regions again shows that the modified ETD schemes with higher order quadrature for the complex integrals do not significantly affect the stability regions to their unmodified counterparts.

The stability regions of the modified ETD4 with different numbers (4, 8, 16, and 32) of quadrature points on circles of various radii are shown in Figure 3.6. These figures suggest that when the radius of the contour circle is not very large, more quadrature points will not improve the stability of the scheme; or, put it in another way, using less quadrature points (even just two points) will

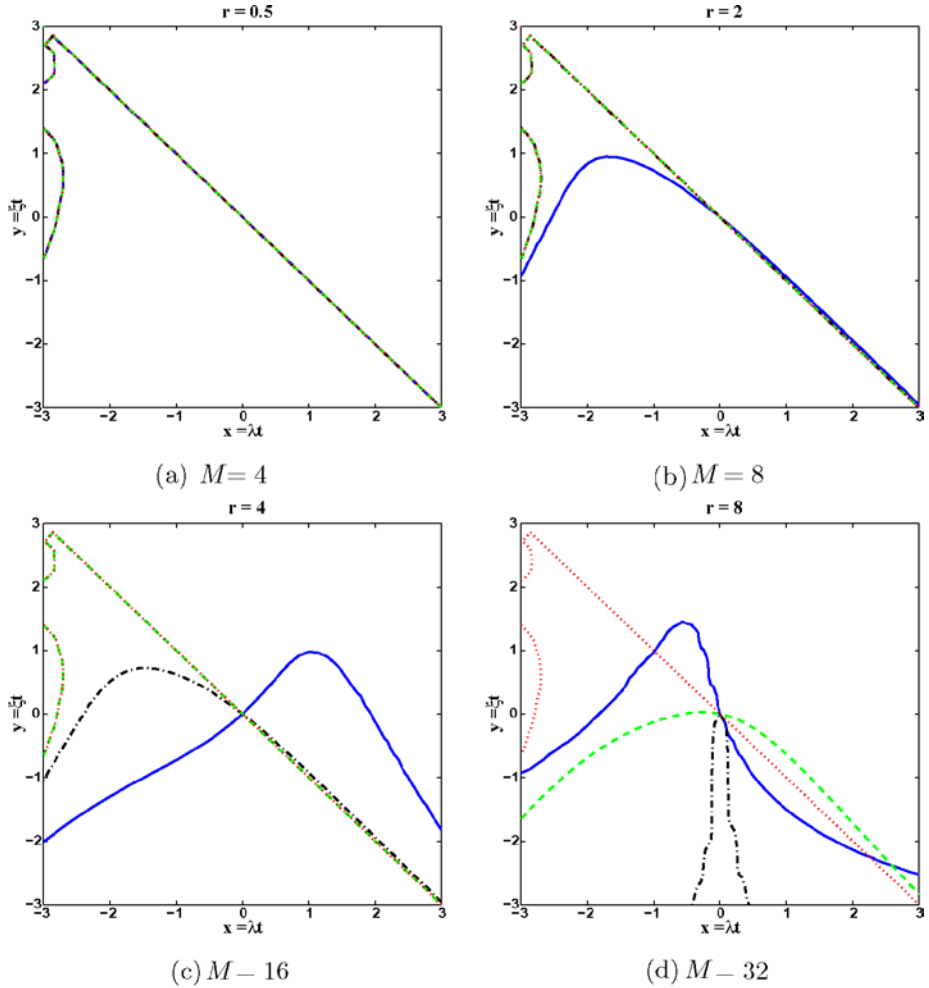


Figure 3.6: Stability regions of modified ETDRK4 schemes in the λt - ξt plane: various number of quadrature points for fixed radius of contour. In (a)–(d), 4, 8, 16, and 32 points are used respectively; and they are shown in solid, dashed–dotted, dashed, and dotted lines respectively.

not significantly degrade the stability of the scheme. The plots in Figure 3.7 also reveal the same fact, in which the stability regions of the modified ETDRK4 are shown for 2 and 16 quadrature points but with different contour radii. In general, the region increases when the radius becomes larger. It is also noticed that if the radius is no more than a quarter of the number of quadrature points, the stability region will not change significantly, and hence it hardly affects the stability of the scheme, although the different choices of the contour radii may affect the accuracy of the numerical contour integration. However, when the radius is greater than about a quarter of the number of quadrature points,

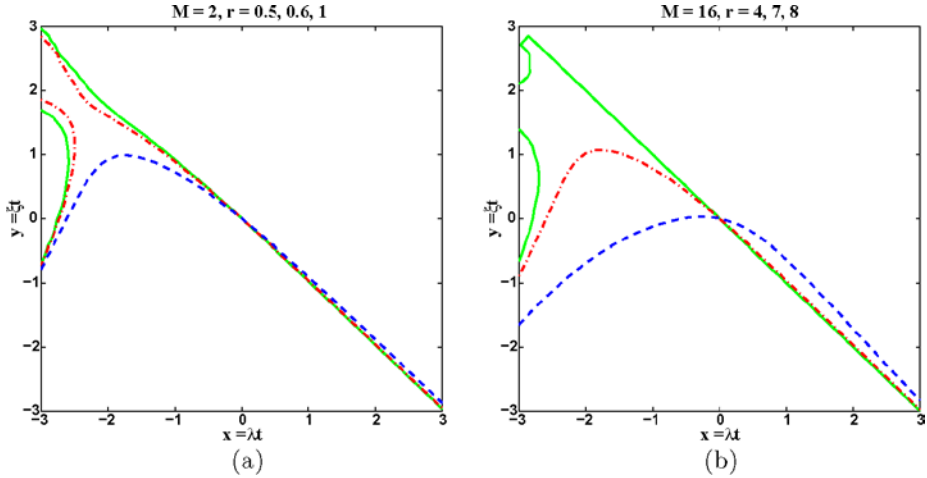


Figure 3.7: Stability regions of modified ETDRK4 schemes in the $\lambda t - \xi t$ plane: various radii of contour circles for fixed number of quadrature points. In (a), $M = 2$ and $r = 0.5, 0.6, 1$; while in (b), $M = 16$ and $r = 4, 7, 8$. In each figure, they are shown in solid, dashed-dotted, and dashed lines respectively.

dramatic change of the stability region tends to occur. The rigorous analysis of this computational observation remains to be carried out.

4 Numerical results.

We now turn our attention to the application of the ETD and modified ETD schemes to the solution of the TDGL equation (2.2), which often forms a core component of the phase field modeling of a binary alloy. The unknown function u represents an order parameter, and the nonlinear term $N(u) = u - u^3$ is obtained from the standard double-well free energy potential [14].

In our simulations, periodic boundary condition is used as it often is the case in practice where the bulk properties are of central interests. This leads, conveniently, to the application of the Fourier pseudospectral approximation in space. In all of our computations, we choose to use the software package FFTW for the discrete fast Fourier transforms (FFT) and inverse fast Fourier transforms (IFFT). At $t = 0$, an initial condition is used which has a circular (spherical) interface boundary centered at the center of a square (cubic) domain. The order parameter values inside the circle (sphere) are assigned $+1$ and -1 outside. Such a circular (spherical) interface is unstable and will undergo the mean curvature motion. Therefore, the circle (sphere) will shrink and eventually disappear.

Consider the equation

$$(4.1) \quad u_t = \Delta u + \frac{1}{\varepsilon^2} u(1 - u^2).$$

If $A(t)$ is the area (volume) of the circle (sphere) at time t with positive u values and A_0 is the initial area, then in the limit as $\varepsilon \rightarrow 0$, that is, in the sharp

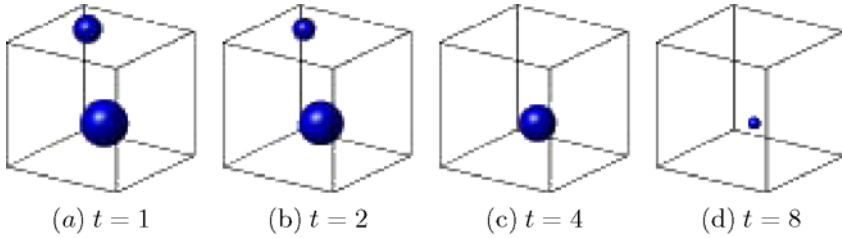


Figure 4.1: Isosurface plots (two disjoint spheres at $t = 0$) with isosurface value $1.0E - 12$.

interface limit, the mean curvature motion gives

$$(4.2) \quad A(t) = A_0 - 2\pi t.$$

Thus, we expect asymptotically that the area (volume) of the solution of (2.2) with positive values will decrease linearly in time until it reaches a terminal time, at which point, the circle (sphere) vanishes. Numerical experiments on the similar problems have been conducted in, for example, [3, 5] and the references cited therein.

For the remaining experiments, we let $\varepsilon = 1$ and take a fixed spatial domain size of 32×32 square and $32 \times 32 \times 32$ cube in two and three-dimensional spaces respectively. We let N denote the number of the spatial grids, or the number of Fourier modes, and set $N = 32, 64$ and 128 . We also take the interface boundaries at $t = 0$ to be two disjoint spheres of radii 6 and 4 respectively; and the order parameter values inside the spheres are assigned $+1$ and -1 outside. Similar snapshots are shown in Figure 4.1. It is seen that the spheres shrink and eventually disappear, and the smaller sphere disappears first. In the computation, a $128 \times 128 \times 128$ grid is used.

For the two-dimensional case with a 64×64 grid, we perform the simulation using semi-implicit method, the modified ETD1, ETDRK2, ETDRK3, and the ETDRK4 schemes (we take 32 quadrature points and the unit circle for the complex contour integration) to compare their accuracy and efficiency.

The terminal times are computed for these schemes with various step sizes. The results are shown in Figure 4.2. It can be seen that for ETDRK4, the variation of the computed terminal time is the least when the step size increases, thus, it overall enjoys better stability and higher accuracy among all the schemes presented. In fact, the ETDRK4 yields the same level accuracy, say 0.1%, as the semi-implicit scheme with step size 50 times smaller. This results in significant increase in computational efficiency: the CPU time for ETDRK4 with the larger step size is about 7% of that for the semi-implicit scheme with the smaller step size.

The computation using ETDRK4 with a very small time step size gives the estimated terminal time at 76.04382. We then find out that to obtain values of the terminal time that fall within a range of 0.1%, 0.25%, 0.5%, 1%, 2.5%, 5%, 7.5%, and 10% to the value 76.04382, the largest step size each scheme can take, then using those step sizes to compute the time it takes for the circular interface

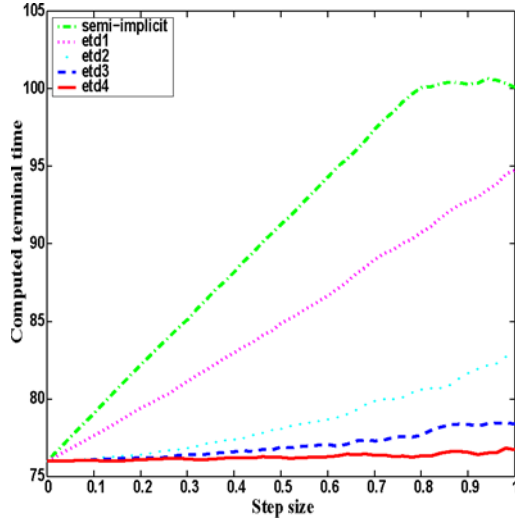


Figure 4.2: Computed terminal times for ETD1, ETDRK2, ETDRK3, and ETDRK4 on a 64×64 grid with various step sizes.

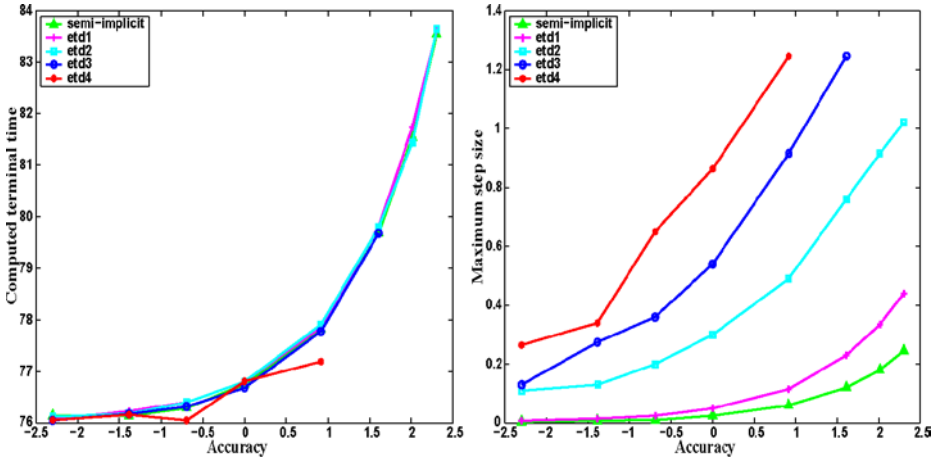


Figure 4.3: Computed terminal times and largest step sizes and vs. accuracy (in logarithmic scale), using 64×64 grids.

to vanish. The results are shown in Figure 4.3 for the 64×64 grid. From the right figure, we see that within the same level of accuracy, ETDRK4 can use the largest step size, ETDRK3 can use the second largest one, the next are ETDRK2 and ETD1 respectively, and the semi-implicit method has the most restricted (the smallest) step size. The smaller the accuracy tolerance level is, the greater the effect on the step size of the modified ETDRK4 is. Both the left and the right figures show better accuracy of modified ETDRK4 than the other schemes.

We also compare the performance and the computational cost of these schemes. In the main time forwarding processes of these schemes, the most intensive CPU

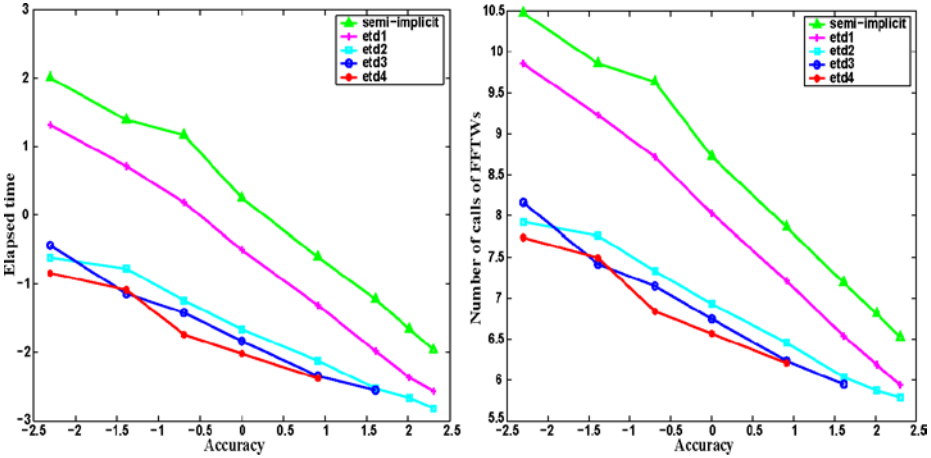


Figure 4.4: CPU times and number of FFTW calls vs. accuracy (all in logarithmic scale), using 64×64 grid.

work is the FFT and IFFT calls from FFTW. Although the higher order modified ETD schemes need more storage than that of the semi-implicit method, and cost more time in storage swapping; however, that amount of work is still much less cost effective since in our computations, the number of the grid points is not relatively very large. It is reasonable for us to use the number of FFTs and IFFTs as an approximate measure for the computational cost. Note that in one step, ETDRK4, ETDRK3, ETDRK2, ETD1, and the semi-implicit scheme needs to call FFTW 8, 6, 4, 2, and 2 times; therefore if using the same step size, the CPU time for the modified ETDRK4, ETDRK3, ETDRK2, ETD1 is about 4 times, 3 times, twice, and the same as that of the semi-implicit methods. The elapsed CPU times and the number of FFTW calls for these schemes are shown in Figure 4.4. We find that if the desired error tolerance level (for the terminal time) is set to be under 2.5%, ETDRK4 has the advantage of using less CPU time and less FFTW calls than others since the using of larger time step size results in fewer number of iterations in the time forwarding, and which reduces the total number of FFTW calls. For example, at a 0.1% accuracy level, ETDRK4 can enlarge the time step about 60 times than the semi-implicit method, and reduce the CPU time by a factor of 17; ETDRK4 can enlarge the time step by a factor of 2.6 than that of the ETDRK2 and reduce the CPU time by a factor of 1.25. When the desired error tolerance is too great, ETDRK4 does not show significant effect on enlarging the time step size (or reducing the number of iterations), and hence shows less improvement on CPU time than other modified ETD scheme. However, all the ETD schemes perform better than the semi-implicit method. Also, a comparison of the left and right figure in Figure 4.4 shows that the CPU times are found to be very consistent with the number of total FFTW calls.

Regarding time step sizes, CPU times and the number of FFTW calls in the solving process, the modified ETDRK4 is clearly favored in most general cases. It is found to be the most stable scheme and it also has the most efficiency if

the error tolerance is set to be small; even at fairly large steps, it still maintains good stability and produces high accuracy. Though it requires more FFTs per step than the lower order modified ETD schemes and semi-implicit scheme, at error tolerance level smaller than 2.5%, its CPU time remains relatively low due to the gain in the large time step size that cuts down the number of FFTW calls.

5 Conclusion.

In this paper, we have established various stability properties of the exponential time differencing schemes and their modifications via complex contour integrations for the numerical solutions of parabolic type equations. Both linear and nonlinear model equations have been considered. The contour integration suggested in [13] has been shown to have the effect of improving the stability of integration in time, and when the parameters are properly chosen, it can also improve the accuracy. When applying to a typical nonlinear model used in phase transition, the ETD type schemes have been shown to be both accurate and efficient. In the future, these schemes will be applied to more complex equations that model phase transition problems in multicomponent materials.

Acknowledgement.

The authors would like to thank Longqing Chen, Jingzhi Zhu and Jie Shen for the help on the subject of the phase field models and their numerical solutions. They also wish to thank the referees for their careful reading of the manuscript and for their helpful comments.

REFERENCES

1. G. Akrivis, M. Crouzeix, and C. Makridakis, *Implicit-explicit multistep methods for quasilinear parabolic equations*, Numer. Math., 82 (1999), pp. 521–541.
2. G. Beylkin, J. M. Keiser, and L. Vozovoi, *A new class of time discretization schemes for the solution of nonlinear PDEs*, J. Comput. Phys., 147 (1998), pp. 362–387.
3. G. Caginalp and E. Socolovsky, *Efficient computation of a sharp interface by spreading via phase field methods*, Applied Mathematics Letters, 2 (1989), pp. 117–120.
4. L.-Q. Chen, C. Wolverton, V. Vaithyanathan, and Z. Liu, *Modeling solid-state phase transformations and microstructure evolution*, MRS Bulletin, 26 (2001), pp. 197–292.
5. L.-Q. Chen and J. Shen, *Applications of semi-implicit Fourier-spectral method to phase field equations*, Comput. Physics Comm., 108 (1998), pp. 147–158.
6. S. M. Cox and P. C. Matthews, *Exponential time differencing for stiff systems*, J. Comp. Phys., 176 (2002), pp. 430–455.
7. Q. Du and W. Zhu, *Stability analysis and applications of the exponential time differencing schemes*, Journal of Computational Mathematics, 22(2) (2004), pp. 200–209.
8. E. Weinan, *Analysis of the heterogeneous multiscale method for ordinary differential equations*, Comm. Math. Sci., 3 (2003), pp. 423–436.
9. W. Gear and I. Kevrekidis, *Projective methods for stiff differential equations: problems with gaps in their eigenvalue spectrum*, SIAM Journal on Scientific Computing, 24 (2003), pp. 1091–1106.
10. W. Gear, I. Kevrekidis, J. Hyman, P. Kevrekidis, O. Runborg, and C. Theodoropoulos, *Equation Free Multiscale Computation: enabling microscopic simulators to perform system-level tasks*, to appear in Communications in the Mathematical Sciences, 2003.

11. W. George and J. Warren, *A parallel 3d dendritic growth simulator using the phase-field method*, Journal of Computational Physics, 177 (2002), pp. 264–283.
12. E. Hairer and G. Wanner, *Solving Ordinary Differential Equations II: Stiff and Differential Algebraic Problems*, Springer-Verlag, New York, 1999.
13. A. Kassam and L. N. Trefethen, *Fourth-order time stepping for stiff PDEs*, SIAM Journal on Scientific Computing, 26 (2005), pp. 1214–1233.
14. A. Khachaturyan, *Theory of Structural Transformations in Solids*, John Wiley, New York, 1983.
15. J. Lambert, *Numerical Methods for Ordinary Differential Systems The Initial Value Problem*, John Wiley and Sons, New York, 1991.
16. D. R. Mott, E. S. Oran, and B. van Leer, *A quasi-steady-state solver for the stiff ordinary differential equations of reaction kinetics*, J. Comp. Phys., 164 (2002), pp. 407–468.
17. P. Yu and Q. Du, *A Variational Construction of Anisotropic Mobility in Phase-Field Simulation*, preprint (2003).
18. J. Zhu and L.Q. Chen, private communications, 2003.